A Novel Environment Characterization Metric for Clustered MIMO Channels Used to Validate a SAGE Parameter Estimator

Nicolai Czink[1,2], Giovanni Del Galdo[3], Xuefeng Yin[4], Ernst Bonek[2], Juha Ylitalo[5,6]

[1]Telecommunications Research Center Vienna (ftw.), Vienna, Austria
[2]Institute of Communications and Radio-Frequency Engineering, Vienna University of Technology, Austria
[3]Ilmenau University of Technology, Communications Research Laboratory, Ilmenau, Germany
[4]Department of Electronics Systems, Aalborg University, Aalborg, Denmark
[5]Centre for Wireless Communications, University of Oulu, Finland
[6]Elektrobit, Finland
E-Mail: czink@ftw.at

Abstract

In this work we introduce a novel metric for characterizing the double-directional propagation environment and use this metric to assess the performance of a SAGE parameter estimator for MIMO channels.

Using the IlmProp, a geometry-based MIMO channel modeling tool, we construct synthetic channels for three different scenarios showing: (i) well separated clusters containing dense propagation paths, and single-bounce scattering; (ii) partly overlapping clusters containing widely spread propagation paths, and single-bounce scattering; (iii) unclustered multipath components ("rich scattering"), and double-bounce-only scattering. We model the scatterers and the receiver in the environment as fixed, but the transmitter as moving.

The Initialization and Search-Improved SAGE estimation tool is used to extract the propagation paths from the constructed channels. Both true and estimated paths are fed to the new system-independent metric which genuinely reflects the structure of the channel and the compactness of the propagation paths. We use this metric to decide on the accuracy of the channel estimator.

The results show a convincing agreement between true and estimated paths.

I. Introduction

Novel MIMO channel models use the concept of clustered propagation paths (e.g. [1], [2], [3]), where these clusters need to be parametrized from measurements. Lately, automatic cluster-finding algorithms have emerged, but they are based on the precondition that the environment is indeed clustered [4]. No metric has been developed yet to judge how "clustered" a propagation environment is. Previously, a metric to quantify the compactness of the direction of paths was introduced in [5], [6], but this metric focuses on distinct ends of the link only. In this paper we extend this concept to the whole double-directional parameter domain, which enables us to judge the compactness of a propagation scenario. The novel *environment characterization metric* is system-independent and allows to characterize the environment in a compact way.

To parametrize cluster-based models, channel parameter estimators are used to extract propagation paths from MIMO measurements, then cluster finding and tracking algorithms try to get hold of cluster parameters. The high-resolution parameter estimators are essential for characterizing the double-directional radio channel, since they allow for estimating individual propagation paths beyond the intrinsic resolution of the measurement system.

These parameter estimators were shown to be well-suited for estimating distinct propagation paths [7], but no analysis was done for clustered paths. Another study described the impact of a low-resolution parameter estimator [8]. Already estimated paths from MIMO measurements were used as input data for generating channel matrices. Subsequently a parameter estimator re-estimated the data. Note that the effects of the initial parameter estimator were already present in the input data, hence this scheme cannot truly judge the true performance of the estimator.

To assess the accuracy of the parameter estimator, which is based on the Initialization and Search-Improved SAGE (ISIS) algorithm [7], we apply it to smoothly time-variant synthetic channels for three different kinds of propagation environments to cover different grades of clustering. Synthetic channels are advantageous for a study of estimator accuracy as the exact location of the propagation paths is known. For generating the channel realizations the IlmProp MIMO channel modelling tool is used.

A comparison between true and estimated paths can be quite tricky, as the parameter estimator typically does not estimate the number of paths correctly, nor does the data model necessarily fit. To make sure that the estimation results describe the propagation environment sufficiently well, it is necessary to assess the accuracy of the channel estimation. The used metric becomes paramount and should reflect the multi-path structure of the true and the estimated channel. We extend the idea of [5], [6] to characterize the environment at both link ends with a single global metric. We achieve this by considering the double-directional and delay domain [9], where paths are characterized by directions of departure, directions of arrival, delays and path weights, and propose to use this metric, which we call environment characterization metric (ECM). This metric is independent of the number of paths and of the system model, which makes it well suited to compare environments by means of propagation paths.

This paper is organized as follows: the novel environment characterization metric is detailed in Section II. Section III describes the framework for the test of the channel estimator. The synthetic environments are presented in Section IV. A short description of the space-alternating generalized expectation-maximization (SAGE) estimator used is given in Section V. Finally we present the results in Section VI and conclude with Section VII.

II. Environment characterization metric

We assume that the environment can be sufficiently described by M subsequent snapshots in time, where each snapshot is described by L_m propagation paths between the transmitter (Tx) and receiver (Rx). The l-th path in the m-th snapshot is described by the path parameter vector $\boldsymbol{\theta}_{ml}$, containing its complex-valued path-weight (γ_{ml}), delay (τ_{ml}), azimuth and elevation of departure ($\varphi_{\mathrm{Tx},ml}$ and $\phi_{\mathrm{Tx},ml}$), and azimuth and elevation of arrival ($\varphi_{\mathrm{Rx},ml}$ and $\phi_{\mathrm{Rx},ml}$), hence

$$\boldsymbol{\theta}_{ml} = [\gamma_{ml}\ \tau_{ml}\ \varphi_{\mathrm{Tx},ml}\ \phi_{\mathrm{Tx},ml}\ \varphi_{\mathrm{Rx},ml}\ \phi_{\mathrm{Rx},ml}]^{\mathrm{T}}, \tag{1}$$

$$l = 1 \ldots L_m, \quad m = 1 \ldots M. \tag{2}$$

All paths in one snapshot are collected in

$$\boldsymbol{\Theta}_m = [\boldsymbol{\theta}_{m1} \ldots \boldsymbol{\theta}_{mL_m}],\ m = 1 \ldots M. \tag{3}$$

Using a system model with specific system parameters and antenna patterns, frequency-dependent channel matrices can be calculated for each snapshot in time.

A. Environment characterization

The new metric is calculated for every single snapshot m, so we will skip this index for better readability. As the metric has to cope with path parameters in different units (angular and delay), it is essential to transform the parameter matrix by proper scaling of its elements. For every path

l, angular data is transformed into coordinates on the unit sphere for both, Rx and Tx. For angles of arrival the transformation is given as

$$\begin{bmatrix} x_{\mathrm{Rx},l} \\ y_{\mathrm{Rx},l} \\ z_{\mathrm{Rx},l} \end{bmatrix} = \frac{1}{2} \begin{bmatrix} \sin\phi_{\mathrm{Rx},l} \cdot \sin\varphi_{\mathrm{Rx},l} \\ \sin\phi_{\mathrm{Rx},l} \cdot \cos\varphi_{\mathrm{Rx},l} \\ \cos\phi_{\mathrm{Rx},l} \end{bmatrix}, \tag{4}$$

for angles at the Tx it reads similarly. The scaling is done such that the maximum Euclidean distance between two paths is limited to 1.

Delay is scaled by the maximum delay that occurs in the considered snapshot [10], hence

$$\tilde{\tau}_l = \frac{\tau_l}{\max_l \tau_l} \tag{5}$$

Every path is now described by seven (dimensionless) parameters collected in

$$\boldsymbol{\pi}_l = [x_{\mathrm{Rx},l}\ y_{\mathrm{Rx},l}\ z_{\mathrm{Rx},l}\ x_{\mathrm{Tx},l}\ y_{\mathrm{Tx},l}\ z_{\mathrm{Tx},l}\ \tilde{\tau}_l]^{\mathrm{T}} \tag{6}$$

and its power $|\gamma_l|^2$. When considering propagation in the azimuthal plane only, the z-direction must be excluded.

The mean parameter vector is then given as

$$\bar{\boldsymbol{\pi}} = \frac{\sum_{l=1}^{L} |\gamma_l|^2 \boldsymbol{\pi}_l}{\sum_{l=1}^{L} |\gamma_l|^2}. \tag{7}$$

We define the novel *environment characterization metric* (ECM) as the covariance matrix of the path parameter vector $\boldsymbol{\pi}$, so that

$$\mathbf{C}_{\boldsymbol{\pi}} = \frac{\sum_{l=1}^{L} |\gamma_l|^2 (\boldsymbol{\pi}_l - \bar{\boldsymbol{\pi}})(\boldsymbol{\pi}_l - \bar{\boldsymbol{\pi}})^T}{\sum_{l=1}^{L} |\gamma_l|^2}. \tag{8}$$

This metric shows the following properties:

- The metric is *system independent* as it is calculated from the propagation paths directly.
- The main diagonal contains the directional spreads of the single components ($x/y/z$) at Rx and Tx and the (normalized) rms delay spread.
- The singular values (SV) of $\mathbf{C}_{\boldsymbol{\pi}}$ can be interpreted as "fingerprint" of the scenario, by which one can judge the compactness of the paths in the channel (see Section VI).
- The trace $\mathrm{tr}\{\mathbf{C}_{\boldsymbol{\pi}}\}$ is the sum of the directional spreads [11] at Rx and Tx plus the (normalized) delay spread. Note that the trace is dominated by the *large* SVs.
- The determinant $\det\{\mathbf{C}_{\boldsymbol{\pi}}\}$ has similar importance as detailed in [5], [6]. It describes the volume spanned in the parameter space. Since the value is dominated by the *small* SVs, it provides information about the most compact domain.

B. Environment mismatch

To quantify the difference between two environments (α) and (β), we first calculate the ECM $\mathbf{C}_{\boldsymbol{\pi}}^{(\alpha)}$ and $\mathbf{C}_{\boldsymbol{\pi}}^{(\beta)}$, and then determine the deviation of all SVs, hence

$$\mathcal{E} = \frac{1}{D} \sum_{d=1}^{D} |\log(\sigma_d^{(\alpha)}) - \log(\sigma_d^{(\beta)})|, \tag{9}$$

where $\sigma_d^{(\alpha)}$ and $\sigma_d^{(\beta)}$ denote the value of the respective SV of the ECM, and D is the number of non-zero SVs.

We provide some intuition about this deviation metric: Assuming $\sigma_d^{(\alpha)} > \sigma_d^{(\beta)}$, the modulus operator can be dropped from (9). Straight-forward calculation leads to

$$\mathcal{E} \sim \log \frac{\det(\mathbf{C}_{\boldsymbol{\pi}}^{(\alpha)})}{\det(\mathbf{C}_{\boldsymbol{\pi}}^{(\beta)})} \tag{10}$$

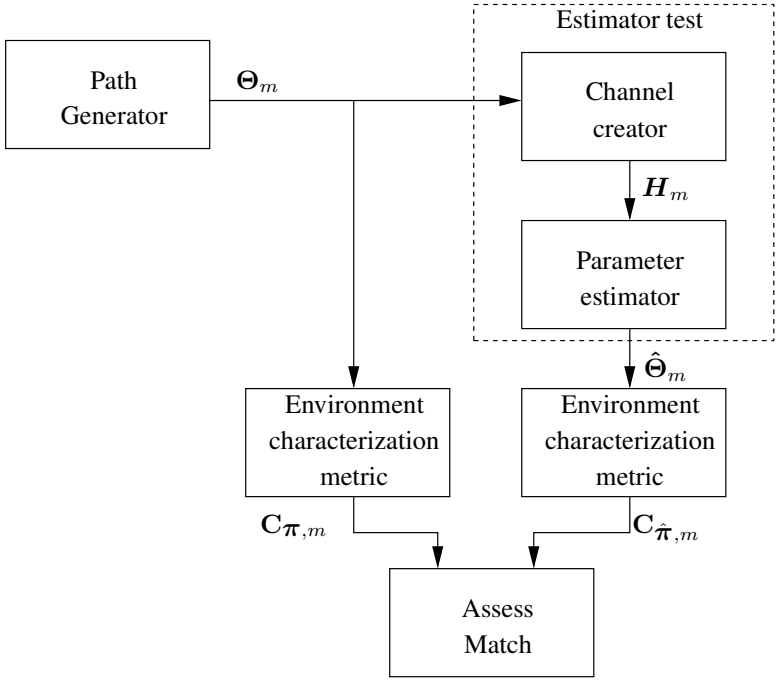

Fig. 1. Framework for assessing estimator performance

This indicates that the difference of the SVs (in dB) can be interpreted as the ratio of the volume that the ECMs span, if the SVs of one scenario are always larger than the other one.
In the Results (see Section VI) we will show the implication of the SVs and how they influence the estimator performance.

III. Validation framework

Validating high-resolution estimation algorithms is difficult for several reasons. First, the data model assumed by the estimator does not necessarily fit the true propagation mechanisms (*model mismatch*). Furthermore, even assuming that the data model were exact, the algorithm could still suffer from a *model order mismatch*, i.e., estimating the wrong number of propagation paths.

In this work we focus on the latter case, where we assume that the true number of paths is larger than the number of estimated ones. However, the framework introduced in this paper can as well be applied to both kinds of deficiencies.

Since the number of estimated paths usually does not match the true number, well-known error metrics like the mean-squared estimation error cannot be applied. Also the "reconstruction error", i.e. the difference between true and (reconstructed) estimated MIMO channel matrix does not reflect properties of the channel well. For this reason we propose to use the ECM, a novel metric to characterize the channel (cf. Section II).

For testing the accuracy of the channel estimator in different environments we use the framework shown in Fig. 1. First, path parameters $\boldsymbol{\Theta}_m$ (cf. (1) and (3)) are generated using the IlmProp channel tool (see Section IV-A). For simplicity we disregard elevation. Using specific system parameters and antenna patterns, frequency-dependent channel matrices $\boldsymbol{H}_m$ are calculated for each snapshot in time.

Then, ISIS is used to estimate the channel parameters (see Section V). The outcome are the estimated parameters $\hat{\boldsymbol{\Theta}}_m$ for each channel snapshot m.

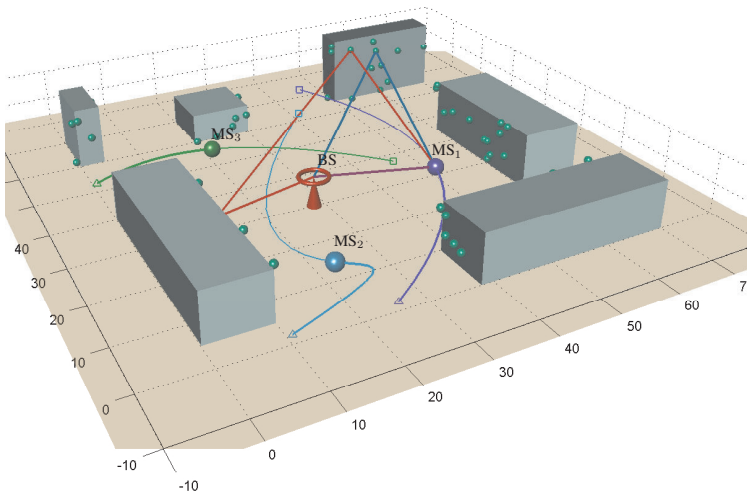

Fig. 2. Sample scenario generated with the IlmProp to illustrate the capabilities of the channel model

The snapshots with the generated paths and with the estimated ones are fed to the ECM. This allows for fair comparison of the true and estimated parameters.

The final outcome describes the match between true and estimated parameters.

IV. Simulated Environments

We use the IlmProp channel modeling tool for generating the environments and for calculating the frequency-dependent channel matrices [12].

A. The IlmProp channel modeling tool

The IlmProp is a flexible geometry-based multi-user MIMO channel modeling tool, capable of dealing with time variant frequency selective scenarios. Its main scope is the generation of channel impulse responses (CIR) as a sum of propagation rays. One or more mobile stations (MS) are modeled in the three-dimensional space by storing their Cartesian coordinates at all time snapshots considered. One base station (BS), which can also be moved in space, represents the other side of the link. The BSs and a MSs can be specified as either a Tx or a Rx, depending on the modeled scenario. Figure 2 illustrates an exemplary IlmProp scenario, where three MSs (MS_1, MS_2, and MS_3) move around the BS. Their curvilinear trajectories are shown. The BS and MSs can employ any number of antennas arranged in an array with arbitrary geometry. The polarimetric radiation patterns of the array elements can be either synthetic or measured, and are stored in form of their effective aperture distribution function [13].

The propagation is modeled as a sum of ray-like paths which link each MSs to the BS. The line of sight (LOS) is the path which connects directly the MS to the BS. Non-line-of-sight (NLOS) components, on the other hand, are modeled by defining a series of point-like interacting objects (IO) through which the path propagates.

The IOs model any interaction of the planar wave with a physical object, such as a reflection or a diffraction. Since an IO does not specify the type of interaction, we refer to it simply as a *scatterer*. To each scatterer, a time variant *scattering coefficient* is assigned. The scattering coefficient determines the percentage of power scattered by the IO towards the next IO or, in case of the last scatterer of a path, towards the receiver. The scattering coefficient refers to (amplitude)

path weight and can also be complex to allow the modeling of a phase shift introduced by the scatterer.

In the scenario shown in Figure 2, the scatterers are placed randomly on the surfaces of several buildings, and are represented by green dots. The figure shows also two paths linking the first MS to the BS. One represents a single-bounce path, the other a double-bounce. The number of paths and which scatterers they travel through are arbitrary and can change at any time instant.

The CIRs are generated by sampling both the time (i.e. snapshot) and frequency domain. After setting up the geometry of the scenario and defining the range and sampling intervals for time and frequency, the IlmProp calculates the channels as a superposition of the LOS path and $\tilde{L}_m - 1$ NLOS paths in the time-frequency domain. For each time snapshot m and path l, the complex path-weight γ_{ml}, delay τ_{ml}, azimuth and elevation of departure ($\varphi_{\mathrm{Tx},ml}$ and $\phi_{\mathrm{Tx},ml}$), and azimuth and elevation of arrival ($\varphi_{\mathrm{Rx},ml}$ and $\phi_{\mathrm{Rx},ml}$), are determined. At the frequency f, the MIMO channel transfer matrix $\boldsymbol{H}_m(f) \in \mathbb{C}^{N_{\mathrm{Rx}} \times N_{\mathrm{Tx}}}$, where N_{Tx} and N_{Rx} are the numbers of transmitting and receiving antennas, respectively, is calculated as

$$\boldsymbol{H}_m(f) = \sum_{l=1}^{\tilde{L}_m} \gamma_{ml}\ \mathrm{e}^{-j2\pi f \tau_{ml}}\ \boldsymbol{a}_{\mathrm{Rx}}(\varphi_{\mathrm{Rx},ml}, \phi_{\mathrm{Rx},ml})\ \boldsymbol{a}_{\mathrm{Tx}}^{\mathrm{H}}(\varphi_{\mathrm{Tx},ml}, \phi_{\mathrm{Tx},ml}), \tag{11}$$

where $\boldsymbol{a}_{\mathrm{Tx}}$ and $\boldsymbol{a}_{\mathrm{Rx}}$ are the transmitting and receiving array response vectors for the plane wave impinging from the azimuth φ and the elevation ϕ, respectively. The superscript $(\cdot)^{\mathrm{H}}$ denotes the Hermitian transpose operator.

At the m-th time snapshot, the complex path weights γ_{ml} can be expressed as

$$\gamma_{ml} = \omega_{ml}\, \rho_{ml}\, \frac{1}{4\pi f \tau_{ml}}, \tag{12}$$

where ρ_{ml} is the product of the scattering coefficients along the l-th path, and ω_{ml} is a boolean variable which is zero if an obstacle is obstructing the path and one otherwise. For the LOS component (i.e., for $l = 1$), $\rho_1 = 1$ and τ_1 is simply the propagation time between the Tx and Rx antenna arrays.

The IlmProp, seen as a modeling tool, allows the generation of a variety of channels – in principle all which can be modeled as a sum of rays. Obviously, the parameters which describe the paths are crucial. In the IlmProp, they can be either retrieved from measurements, implementing the so-called Measurement Based Parametric Channel Modeling concept [14], or input manually.

In the latter case, assuming that the user inputs a realistic propagation scenario, the IlmProp will model realistically the correlation in time, frequency and space, which are inherent to the model, i.e., they are a direct consequence of the geometry defined.

B. Modeled Scenarios

We decided to compare the accuracy of channel estimation for three different types of scenarios (see Fig. 3) showing (a) well separated clusters containing dense propagation paths, and single-bounce scattering; (b) partly overlapping clusters containing widely spread propagation paths, and single-bounce scattering; (c) unclustered multipath components (“rich scattering”), and double-bounce-only scattering.

For this application, the IlmProp is a well suited tool, as it gives us the possibility to input the paths trajectory explicitly, making it possible to obtain the CIRs for the scenarios above mentioned with little effort. The scenarios are shown in Fig. 3, where the red ball denotes the position of the Rx array, the blue ball denotes the Tx array at its final point, the blue line shows the Tx route, and the green circles indicate scatterers. The channels were generated for a bandwidth of 100 MHz, with 510 frequency samples. The Tx employs a Uniform Linear Array with 15 sensors 0.45 wavelengths spaced and slightly directive beam patterns. The Rx employs a Uniform Circular

Array with 15 sensors 0.4 wavelengths spaced and slightly directive beam patterns. Only vertical-to-vertical polarization is considered. No noise was added in any of the three scenarios.

For Scenario (a), 70 single-bounce scattering paths were assumed, in Scenario (b), we used 80 single-bounce paths, whereas for the rich-scattering scenario in Fig. 3(c), 100 double-scattering paths occur, where always two scatterers were picked out randomly of the scenario to form one double-scattering path. The latter scenario is quite unrealistic, but serves well as worst-case example for rich scattering.

V. Channel parameter estimator

We applied the Initialization and Search-Improved SAGE (ISIS) algorithm [7] to the synthetic data generated by IlmProp for the different scenarios. The ISIS algorithm is an improvement of the SAGE algorithm [15] in terms of convergence speed, detection ability of the weak paths and computational effort [16]. The unknown path parameters are estimated using the individual snapshots of the channel matrix in the delay domain. Since we perform the estimation for every snapshot m, we drop this index in this section for better readability. We denote the snapshot of the channel matrix using $\boldsymbol{h}(\tau)$. Notice that the output of the IlmProp are the snapshots of the (frequency-domain) channel transfer matrix $\boldsymbol{H}(f)$. To obtain $\boldsymbol{h}(\tau)$ we use the inverse discrete Fourier transformation. In the sequel we briefly describe the signal model and the ISIS algorithm. For more details of this algorithm, the readers are referred to [15] and [7].

A. Signal model

We consider each snapshot of the propagation environment to consist of L paths. So, we obtain the model of the channel matrix $\boldsymbol{h}(\tau)$ as

$$\boldsymbol{y}(\tau) = \underbrace{\sum_{l=1}^{L} \boldsymbol{s}(\tau;\boldsymbol{\theta}_l)}_{\boldsymbol{h}(\tau)} + \boldsymbol{w}(\tau), \tag{13}$$

where $\boldsymbol{y}(\tau)$ denotes the observation of the channel matrix, and $\boldsymbol{s}(\tau;\boldsymbol{\theta}_l)$ is the path response representing the contribution of the l-th path to $\boldsymbol{h}(\tau)$, which can be written as

$$\boldsymbol{s}(\tau;\boldsymbol{\theta}_l) \doteq \gamma_l p(\tau-\tau_l)\ \boldsymbol{a}_{\mathrm{R}}(\varphi_{\mathrm{Rx},l},\phi_{\mathrm{Rx},l})\ \boldsymbol{a}_{\mathrm{T}}^{\mathrm{H}}(\varphi_{\mathrm{Tx},l},\phi_{\mathrm{Tx},l}). \tag{14}$$

In the delay response of a path, we have to account for the limited bandwidth and the sampling by letting

$$p(\tau) = \frac{\sin(\pi\Delta f M_f \tau)}{M_f \sin(\pi\Delta f \tau)},$$

where Δf represents the spacing of two consecutive frequencies. In (13), $\boldsymbol{w}(\tau)$ denote a white Gaussian noise process[1] with variance σ_w^2. Based on this model we derive the ISIS algorithm.

B. Theory

The problem is to estimate the parameter vector $\boldsymbol{\Theta}$ in (3) given the observations of $\boldsymbol{h}(\tau)$. A standard method showing good performance would be the maximum likelihood estimator (MLE). However, because of its high computational complexity, it is impractical to implement in real applications.

The ISIS algorithm provides a low-complexity approximation of the MLE with an iterative scheme based on the SAGE concept. The general idea in order to reduce complexity, is to iteratively re-estimate the parameters of every single path $\boldsymbol{\theta}_l$, while fixing the parameters of the other paths,

[1]Note that in our observation model, $\sigma_w^2 = 0$.

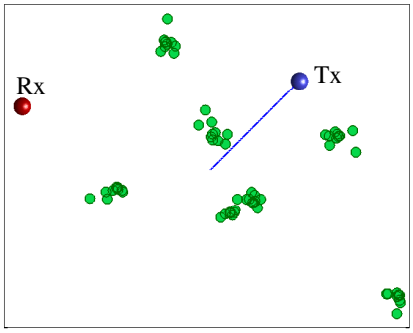

(a)

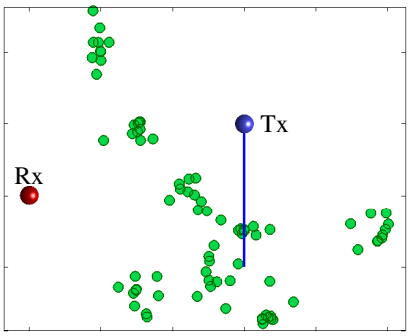

(b)

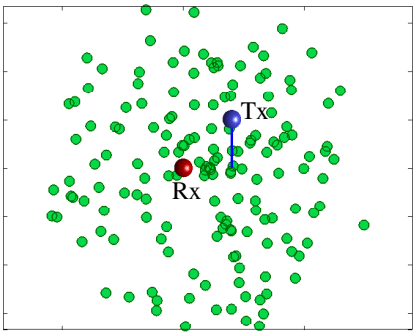

(c)

Fig. 3. Scenarios used for comparing the estimator performance: (a) few clustered paths, (b) larger clusters, (c) rich scattering. The blue lines indicate the trajectories of the transmitter.

in contrast to estimating the parameters of all paths on a whole. The initial values of the parameter estimates $\hat{\boldsymbol{\Theta}}$ are computed using a non-coherent MLE method [17].

In order to re-estimate $\boldsymbol{\theta}_l$, we need to define a data space which provides sufficient information for its estimation. This data space, usually unobservable, is referred to as the "admissible hidden data space" with respect to $\boldsymbol{\theta}_l$. We define this data space as the path response of the l-th path distorted by noise, i.e.

$$\boldsymbol{x}_l(\tau) = \boldsymbol{s}(\tau; \boldsymbol{\theta}_l) + \tilde{\boldsymbol{w}}(\tau). \tag{15}$$

Theoretically, the estimates of $\boldsymbol{\theta}_l$ should be calculated by maximizing its likelihood function, given the admissible hidden data. However, since this data is unavailable ("hidden"), the likelihood function cannot be calculated. To solve the problem, we use an iterative procedure.

In every iteration i, we perform the following two steps for every path parameter subset $\boldsymbol{\theta}_l$:

1. We compute the expectation of the likelihood function of the path parameters $\boldsymbol{\theta}_l$ conditioned on the observation of $\boldsymbol{h}(\tau)$. Then we substitute the true parameters with their estimates. This leads to the objective function

$$Q_l^{[i]}(\boldsymbol{\theta}_l) = -\sum_{\tau=1}^{N_\tau} \left\| \hat{\boldsymbol{x}}_l^{[i]}(\tau) - \boldsymbol{s}(\tau; \boldsymbol{\theta}_l) \right\|_{\mathrm{F}}^2, \tag{16}$$

   where $\|\cdot\|_{\mathrm{F}}$ represents the Frobenius norm and

$$\hat{\boldsymbol{x}}_l^{[i]}(\tau) = \boldsymbol{h}(\tau) - \sum_{l'=1, l' \neq l}^{\hat{L}} \boldsymbol{s}(\tau; \hat{\boldsymbol{\theta}}_{l'}^{[i-1]}) \tag{17}$$

   is the estimate of the admissible hidden data $\boldsymbol{x}_l(\tau)$ given $\boldsymbol{h}(\tau)$, and $\hat{\boldsymbol{\theta}}_{l'}^{[i-1]}$ denotes the parameter estimates obtained in the $(i-1)$ iteration. Note that the estimate of the admissible hidden data with respect to $\boldsymbol{\theta}_l$ is the remainder of the observed channel after subtracting the other estimated paths.
   This step is referred to as the expectation (E-) step.
2. The parameters in the subset $\boldsymbol{\theta}_l$ are re-estimated by maximizing the objective function with respect to $\boldsymbol{\theta}_l$,

$$\hat{\boldsymbol{\theta}}_l^{[i]} = \arg\max_{\boldsymbol{\theta}_l} Q_l^{[i]}(\boldsymbol{\theta}_l). \tag{18}$$

   By applying a coordinate-wise updating procedure as described in [16], this multiple-dimensional maximization can be reduced to multiple one-dimensional maximization problems. This step is called maximization (M-) step of the iteration.

This iterative procedure stops when the likelihood of $\hat{\boldsymbol{\Theta}}$ given the observation $\boldsymbol{h}(\tau)$ reaches its maximum. The last obtained parameter estimates are then the final estimates of $\hat{\boldsymbol{\Theta}}$.

C. Implementation

For the implementation of the ISIS algorithm, we chose the number of propagation paths to be estimated, $\hat{L}$, to be 40 and set the maximum dynamic range for the amplitude of the estimated path weights to 25dB. Note that this number is less than the number of paths used in generating all three synthetic scenarios. Still, using these settings, the ISIS algorithm should be able to capture the dominant paths in the considered environment. In the M-step we selected quantization steps of respectively 0.5 ns in delay and 0.1° in azimuth and elevation. Twenty iteration cycles are performed to extract the parameter estimates.

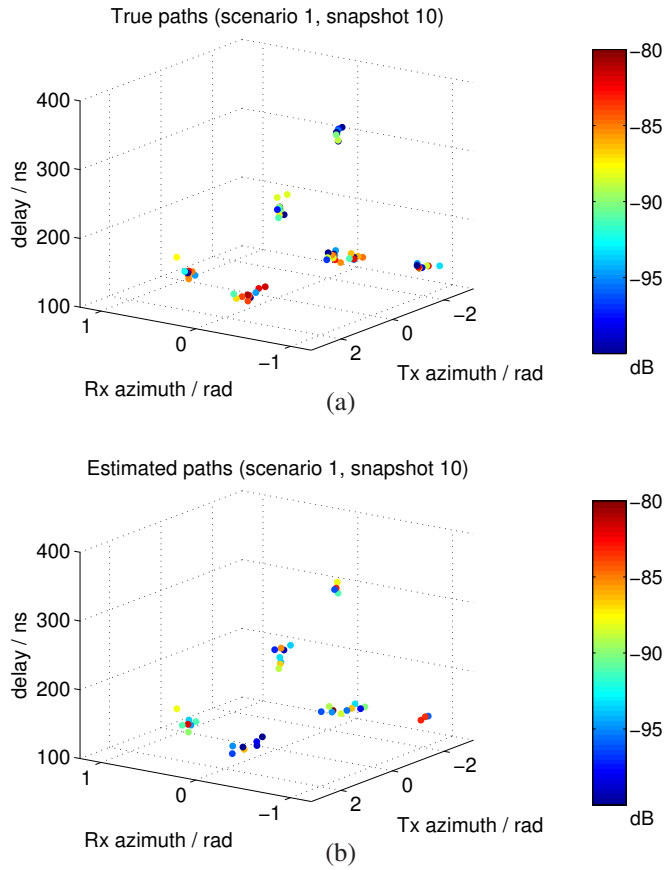

Fig. 4. Visual comparison of true and estimated parameters.

VI. Results

To check whether the signal models used for generating the synthetic data and in the ISIS estimator fit, we conducted a one-path experiment. The model created a channel with only one propagation path showing arbitrary parameters, which were consecutively estimated by the channel estimator. We found that the channel estimator was able to exactly identify the parameters of the single propagation path without a residual error, leading to the conclusion that the signal models are identical and that the estimator works correctly.

To give a first impression of the accuracy of the parameter estimator in a multipath scenario, Fig. 4 shows the true and estimated paths in the parameter domain for one time snapshot of the first scenario. One can observe that the estimator seems to be well able to capture the properties of the environment, even if the number of estimated paths is lower than the true number of paths.

When paths are closer to each other in parameter space than the resolution of the estimator, the parameters cannot be resolved accurately[2]. The estimator rather tries to approximate the path response in the channel matrix by multiple estimated paths. This leads to the effect, that, first a path with strong power is estimated at the centroid of a cluster, then the estimator approximates the paths around the center. This also leads to a different number of estimated paths. For this reason, the estimated path powers as well as the estimated locations of the paths do not coincide with the

[2]Note that this effect occurs regardless of the correct choice of the model order.

TABLE I
MEAN DEVIATION OF THE PARAMETER ESTIMATOR

Scenario	Mean deviation $\bar{\mathcal{E}}$
Scenario 1	1.41 dB
Scenario 2	0.99 dB
Scenario 3	2.78 dB

real paths in general, still the estimator rather resolves the *clusters of paths* quite accurately and the general multipath structure of the scenario is rendered quite accurately.

To assess this statement, we chose to evaluate the estimator by using the ECM. For each scenario we calculated the ECM for the m-th snapshots for the true and estimated paths denoted by $\mathbf{C}_{\boldsymbol{\pi},m}$ and $\mathbf{C}_{\hat{\boldsymbol{\pi}},m}$, and the respective singular values (SV) σ_{md} and $\hat{\sigma}_{md}$, where $d = 1 \dots D$.

Fig. 5 shows these SVs in dB for the three different scenarios. The values for the true paths are indicated by black lines, the estimated paths by red lines and the different SVs by different marker types.

To discuss the significance of the new metric, we first focus only on the true paths results. In Fig. 5(a) one can observe a large distance between the second and third SV, and between the 4th and 5th SV, where especially the last value of Scenario 1 changes strongly over time. Fig. 5(b) show also a large distance between the SVs. In Fig. 5(c) the SVs are very close to each other and do not change significantly. This gives rise to the following conjecture:

> *The distances between the SVs of the environment characterization matrix $\mathbf{C}_{\boldsymbol{\pi}}$ provide information about the compactness of the paths in the environment.*

This means that this metric is able to quantify how clustered a scenario is.

To assess the performance of the parameter estimator, we compare the SVs of the ECM gained from the estimated paths (red/lighter lines) with the ones gained from the true paths (see Fig. 5).

For the first two environments with clustered propagation paths, one can observe that the general trend is the same, but the curves seem to vary around the correct value. The reason for this is the destructive/constructive interference of different paths at the Rx, which attenuates some paths and amplifies others.

In the third (rich scattering) environment the SVs are typically underestimated, which indicates that the true propagation paths are spread wider than the estimated paths. In this instance, the parameter estimator suffers from the model order mismatch, a larger number of paths would be necessary to reflect the scenario correctly. The difference between single-bounce and double-bounce scattering does not affect the estimator quality, since, due to the missing noise in the model, the path loss is not limiting the dynamic range of the estimator.

To quantify the deviation of the estimator we use the *mean* deviation of all SVs over all snapshots from the true value, hence

$$\bar{\mathcal{E}} = \frac{1}{K} \sum_{m=1}^{M} \mathcal{E}_m \tag{19}$$

where $\mathcal{E}_m$ is the mismatch (9) between the m-th modeled and m-th estimated snapshot of the channel.

The mean errors for the three considered scenarios are given in Table I. Interestingly, the values for the first two scenarios are quite similar, but the deviation is larger for the rich-scattering environment.

VII. CONCLUSIONS

We presented the *environment characterization metric* (ECM), a novel metric for characterizing the double-directional propagation environment, which we use to assess the performance of a high-

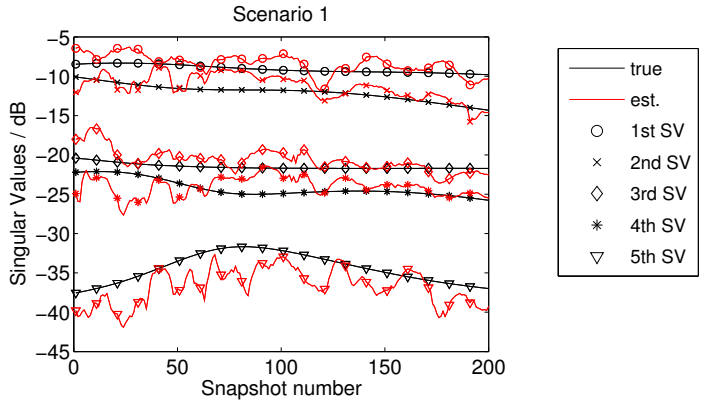

(a)

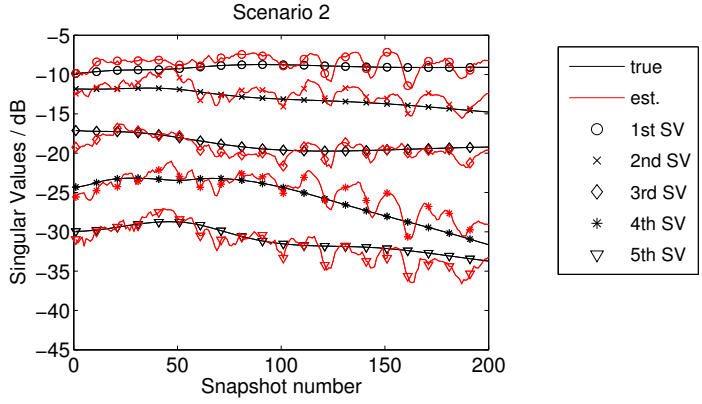

(b)

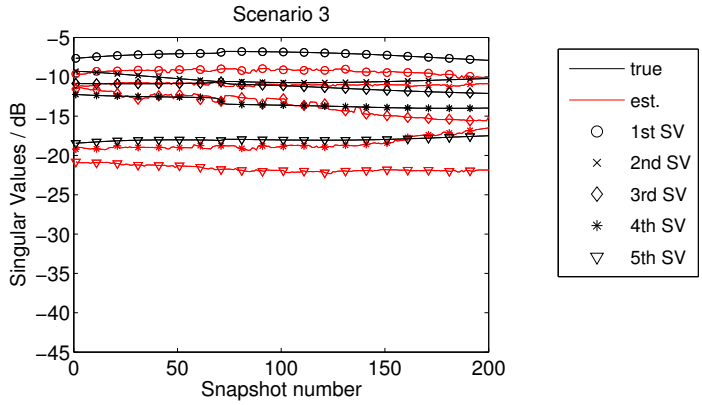

(c)

Fig. 5. Singular values of the environment characterization metric $\mathbf{C}_{\boldsymbol{\pi}}$ for the true and estimated parameters from the three scenarios.

resolution parameter estimator.

The ECM is calculated from the propagation paths directly, hence it is *system independent*. It reflects the compactness of the paths and thereby gives a "fingerprint" of the environment. The metric provides manifest intuition about how clustered a scenario is.

When comparing the fingerprints for true and estimated scenarios, we derived a criterion for the goodness of a parameter estimator. To demonstrate the significance of the ECM, we assess the quality of the ISIS (Initialization and Search-Improved SAGE) parameter estimator. We use the estimator on synthetic channels from different scenarios generated by the IlmProp channel model and compare the results using the metric.

Simulations show that the ECM is well able to characterize the environments and to quantify how clustered a scenario is. Furthermore, we found that the ISIS algorithm is suitable for reflecting the true environment, with better performance for clustered scenarios than for rich scattering (unclustered) ones.

ACKNOWLEDGEMENTS

This work was conducted within the European Network of Excellence for Wireless Communications (NEWCOM). We thank Elektrobit for allowing us to use their implementation of the channel parameter estimator. This paper was supported by the Austrian Kplus program.

REFERENCES

[1] L. Correia, Ed., *Mobile Broadband Multimedia Networks*. Academic Press, 2006.

[2] G. T. 25.996, "3rd generation partnership project; technical specification group radio access network; spatial channel model for MIMO simulations (release 6)," v6.1.0.

[3] H. El-Sallabi, D. Baum, P. Zetterberg, P. Kyösti, T. Rautiainen, and C. Schneider, "Wideband spatial channel model for MIMO systems at 5 GHz in indoor and outdoor environments," in *Proc. IEEE VTC'06 Spring*, Melbourne, Australia, May 2006.

[4] N. Czink, E. Bonek, L. Hentilä, J.-P. Nuutinen, and J. Ylitalo, "Cluster-based MIMO channel model parameters extracted from indoor time-variant measurements," in *IEEE GlobeCom 2006*, San Francisco, USA, November 2006.

[5] A. Pal, M. Beach, and A. Nix, "A quantification of 3-d directional spread from small-scale fading analysis," in *COST 273 Post-Project Meeting*, Lisbon, Portugal, Nov. 2005.

[6] ——, "A quantification of 3-d directional spread from small-scale fading analysis," *IEEE International Conference on Communications*, June 2006, Istanbul, Turkey.

[7] B. H. Fleury, X. Yin, P. Jourdan, and A. Stucki, "High-resolution channel parameter estimation for communication systems equipped with antenna arrays," *Proc. 13th IFAC Symposium on System Identification (SYSID 2003), Rotterdam, The Netherlands*, no. ISC-379, 2003.

[8] M. Mustonen, P. Suvikunnas, and P. Vainikainen, "Reliability analysis of multidimensional propagation channel characterization," in *WPMC*, Aalborg, Denmark, 2005.

[9] M. Steinbauer, A. Molisch, and E. Bonek, "The double-directional radio channel," *IEEE Antennas and Propagation Magazine*, vol. 43, no. 4, pp. 51 – 63, Aug. 2001.

[10] M. Steinbauer, H. Özcelik, H. Hofstetter, C. Mecklenbräuker, and E. Bonek, "How to quantify multipath separation," *IEICE Trans. Electron.*, vol. E85, no. 3, pp. 552–557, March 2002.

[11] B. H. Fleury, "First- and second-order characterization of direction dispersion and space selectivity in the radio channel," *IEEE Transactions on Information Theory*, vol. 46, no. 6, pp. 2027–2044, September 2000.

[12] G. Del Galdo, M. Haardt, and C. Schneider, "Geometry-based channel modelling of MIMO channels in comparison with channel sounder measurements," *Advances in Radio Science – Kleinheubacher Berichte*, pp. 117–126, October 2003, more information on the model, as well as the source code and some exemplary scenarios can be found at *http://tu-ilmenau.de/ilmprop*.

[13] M. Landmann and G. Del Galdo, "Efficient antenna description for MIMO channel modelling and estimation," *European Microwave Week, Amsterdam, The Netherlands*, 2004.

[14] R. S. Thomä, D. Hampicke, M. Landmann, A. Richter, and G. Sommerkorn, "Measurement-based channel modelling (MBPCM)," *ICEAA, Torino*, September 2003.

[15] B. H. Fleury, M. Tschudin, R. Heddergott, D. Dahlhaus, and K. I. Pedersen, "Channel parameter estimation in mobile radio environments using the SAGE algorithm," *IEEE Journal on Selected Areas in Communications*, no. 3, pp. 434–450, 17 1999.

[16] B. H. Fleury, X. Yin, K. G. Rohbrandt, P. Jourdan, and A. Stucki, "Performance of a high-resolution scheme for joint estimation of delay and bidirection dispersion in the radio channel," *Proc. IEEE Vehicular Technology Conference, VTC 2002 Spring*, vol. 1, pp. 522–526, may 2002.

[17] X. Yin, B. H. Fleury, P. Jourdan, and A. Stucki, "Polarization estimation of individual propagation paths using the SAGE algorithm," in *Proceedings of the IEEE International Symposium on Personal, Indoor and Mobile Radio Communications (PIMRC)*, Beijing, China, Sept. 2003.